

Ion-induced Auger-electron emission from aluminum

R. A. Baragiola, E. V. Alonso, and H. J. L. Raiti

Centro Atómico Bariloche and Instituto Balseiro,† 8400-Bariloche, Argentina*

(Received 6 August 1981)

We have observed Al $L_{2,3}$ Auger electrons from clean aluminum surfaces bombarded by mass-analyzed beams of noble-gas ions at 45° incidence, and in the energy range 600 eV–15 keV. The electron energy spectra show a wide structure similar, though not identical, to that observed under electron impact, and sharp lines. These lines are identified as resulting from the Auger decay of $2p$ -excited Al and Al^+ . The decay occurs in vacuum from sputtered particles, as suggested by the asymmetric Doppler broadening of the Auger lines. The Auger yields can be scaled when plotted against the maximum energy transfer in a projectile-Al collision, indicating that the excitation occurs mainly in symmetric collisions between target atoms. Exceptions are the cases of impact with He^+ and low-energy Ne^+ ions where projectile-Al collisions are responsible for the excitation, possibly by two-electron transitions.

I. INTRODUCTION

Collisions of keV ions with solids produce, among other things, the ejection of electrons. In the tail of the energy distribution of these emitted electrons one can notice, in certain cases, Auger electrons from the filling of inner-shell vacancies in the projectile and target atoms.

Early interest in the study of this ion-induced Auger-electron emission (IAEE) from solids, arose for different reasons. In 1960, Parilis and Kishinevskii¹ proposed that Auger processes were the main source of *all* emitted electrons, a model which was recently proved to be incorrect.^{2–5} Snoek *et al.*⁶ observed Ar L -shell electrons under bombardment of gold targets with Ar ions, thus providing one of the first proofs of a prediction of the Fano-Lichten⁷ electron-promotion model for inner-shell excitations in collisions of slow heavy atoms. Joyes and Castaign⁸ proposed that sputtered ions can result from the Auger deexcitation in vacuum of inner-shell excited target atoms. The accompanying Auger electrons were then observed by Hennequin *et al.*^{9,10} for Be, Al, and Si bombarded by keV noble-gas ions, while Joyes *et al.*^{11–13} studied theoretical aspects of the phenomenon. Since then, many workers have studied IAEE for its intrinsic interest, and also to understand its influence in the charge-state distribution of ions backscattered from and transmitted through solids.^{14–17} Studies of IAEE have also been aimed toward the evaluation of theories of inner-shell ionization,^{18,19} and toward the derivation of attenua-

tion lengths of Auger electrons in solids.²⁰

Together with the development of this topic, there appeared contradictory ideas, presented by different workers, about the origin of the Auger electrons, and on the information carried by them. Our aim in this study was to resolve these controversies based on new measurements taken under well-defined conditions. In particular, we were concerned with the following questions:

- (1) Are the inner-shell excitations leading to IAEE produced mainly in collisions between the incident ions and target atoms, or in symmetric collisions between target atoms in the collision cascade in the solid?
- (2) Do the observed Auger lines originate from the deexcitation of atoms inside or outside the solid?

The experimental work, which is presented in Sec. II consisted of measurements of target L_{VV} Auger spectra and yields from clean aluminum samples bombarded by noble-gas ion over the energy range 0.7–15 keV. These results are then discussed in Sec. III, where we address the questions posed above. Finally we point out, in Sec. IV, unsolved problems and promising lines for future research.

II. EXPERIMENTS

A. Apparatus

To perform the observations we used a commercial ultrahigh vacuum equipment equipped with

several surface spectroscopic facilities.²¹ The part relevant for the present work is shown schematically in Fig. 1. The target is a polished disk of high-purity aluminum and is mounted in a carousel inside a mu-metal chamber maintained routinely at a base pressure of less than 3×10^{-11} Torr. The sample was cleaned by sputtering with 2-keV Ar or Ne ions until Auger analysis (AES) using 3-keV exciting electrons showed that surface impurities amounted to less than the equivalent of 1% of a monolayer, and were of no significance in the studies of IAEE.

The ions used in this work were incident at 45° with respect to the normal to the target surface. The ions were produced by an electron bombardment ion source and mass analyzed by a Wien filter. This mass filter also provided deflection of the ions onto the target and thus avoided contamination of the beam with non-mass-analyzed neutrals, a problem present in conventional on-axis devices. During operation of the differentially pumped ion source, the pressure of the noble gas used was in the 10^{-8} -Torr range inside the target chamber; the partial pressure of contaminant gases was 2 orders of magnitude smaller. Periodic tests were made using AES to ascertain that the target was sufficiently clean for making meaningful measurements. The ion energy was known to within $\pm(0.1\% + 2 \text{ eV})$, and the ion current was determined before and after each run with proper electron suppression.

The ejected electrons were detected within a narrow cone 15° from the surface normal, in a plane perpendicular to that of Fig. 1. The area of acceptance on the target surface was larger than that of the ion beam spot. The source of electrons was imaged by a lens onto the entrance slit of a spheri-

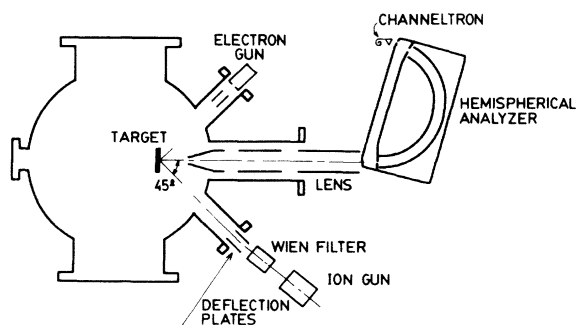


FIG. 1. Schematic diagram of the equipment used. The ion gun is differentially pumped, and the spectrometer is aimed at the target at an angle of 15° from the plane of the figure.

cal sector electrostatic analyzer operating at a constant pass energy and with an energy resolution of 0.4 eV FWHM.

The energy diagram appropriate for the measurements is depicted in Fig. 2. In order that the results transcend the apparatus used, it is necessary to measure the work function of the spectrometer, ϕ_s . This was done by bombarding the target with electrons accelerated through a potential V_f and by measuring the spectrometer voltage V_s required to pass the peak of the energy distribution of the electrons backscattered elastically from the target. Thus,

$$\phi_s = eV_f - eV_s + \phi_f + E_{kT},$$

where e is the charge of the electron, E_{kT} the most probable excess thermal energy of the electrons emitted from the filament at temperature T , and ϕ_f the work function of the filament. For our experimental situation of a tungsten emitter at about 2700 K, $\phi_f + E_{kT} = 4.8 \text{ eV}$, to within 0.1 eV.²²

The spectrometer pass energy is $eV_s = eV_r + CV_p$, where eV_r is the energy by which the electrons are retarded before analysis, C the geometrical constant of the analyzer, and V_p the voltage between the plates of the analyzer. C was determined by tuning on the peak of elastically reflected electrons, and by measuring the required interplate voltage V_p as a function of the retarding voltage V_r . As a result of the calibration, the energy of the electrons with respect to the Fermi level of the sample is

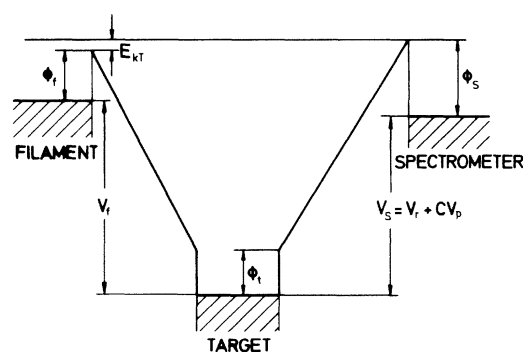


FIG. 2. Electron energy diagram appropriate to the calibration of the electron energy scale, and the measurement of the analyzer work function ϕ_s . E_{kT} and ϕ_f are the most probable excess thermal energy and the work function for the tungsten filament, respectively. V_f is the voltage applied between the filament and the target, V_r the retarding voltage applied to the emitted electrons before analysis by the spectrometer which is set at a pass voltage V_p and has a geometrical constant C . ϕ_t is the work function of the Al target.

known to within ± 0.1 eV.

The electrons were detected with a channel electron multiplier and the data acquisition was performed under computer control using signal-averaging techniques.

B. Electron energy spectra

Figure 3 shows a representative spectrum of electrons in the energy region of the $L_{2,3}$ Auger transitions in aluminum. One can observe two main types of structure. A broad one which resembles that obtained under electron bombardment, and sharp peaks. The broad structure, which we shall call "bulk" following other workers, is very similar, though not identical, to the $L_{2,3}VV$ structure resulting from electron bombardment. The sharp peaks will be denoted "atomic" since their widths are much smaller than what would result if the broad (~ 11 eV) valence band of the solid had been involved in the transition. At higher ion energies small peaks appear at high electron energies which correspond to Auger transitions involving Al atoms with two vacancies in the $2p$ shell.

C. Effects of ion energy

With increasing ion energy there is a dramatic increase in the Auger signals, the growth of the atomic peaks is larger than that of the bulk structure, and the widths of the atomic peaks increase.

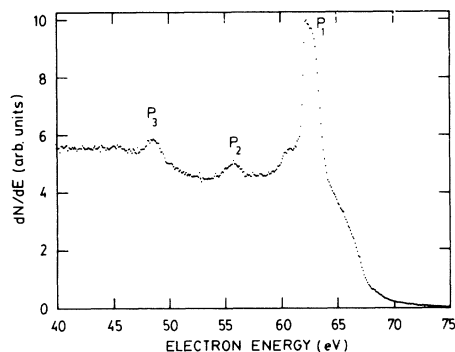


FIG. 3. Electron energy distribution of Al under bombardment with 4-keV Ar^+ ions. The spectrum was measured with the analyzer in the constant retard-ratio mode with a resolution of 0.2%, and corrected for the energy-dependent analyzer transmission function. The work function of the analyzer for this spectrum was measured to be $\phi_s = 4.70$ eV.

A closer look shows no significant variation in the relative heights of the different single-vacancy atomic peaks, nor in the shape of the bulk transition. A new finding of this work is that the broadening is asymmetric, it occurs towards the high-energy side of the peaks, as shown in Fig. 4. As we shall see later, this has implications for the understanding of the origin of the atomic Auger peaks.

It is of interest to get quantitative information on these effects. To this end, it is convenient to separate the atomic from the bulk structure, and the contribution of inelastic scattered electrons from the bulk intensity. The first can be done readily with an estimated error of less than 30% caused by uncertainties in drawing the $L_{2,3}VV$ "background." The separation of the inelastically scattered electrons is more difficult.^{23,24} We circumvent the problem by taking the channel intensity at an arbitrary energy away from the atomic peaks as a measure of the total $L_{2,3}VV$ strength since the shape of the line does not vary with energy. A small correction is done to this intensity by subtracting the extrapolated high-energy background.

In Figs. 5–7 we present the variation of three quantities with ion energy: (a) Y , the atomic Auger yield; (b) R , the ratio of the area of the atomic peaks to the intensity of the bulk line at 60 eV (it is in units of energy); (c) ΔE , the full width at half maximum of the main atomic Auger line. These quantities are shown as functions of projectile energy E_p , and of the scaled energy γE_p , which is the maximum energy that can be transferred in a collision between a projectile of mass m and an Al atom of mass M , where $\gamma = 4mM(m+M)^{-2}$.

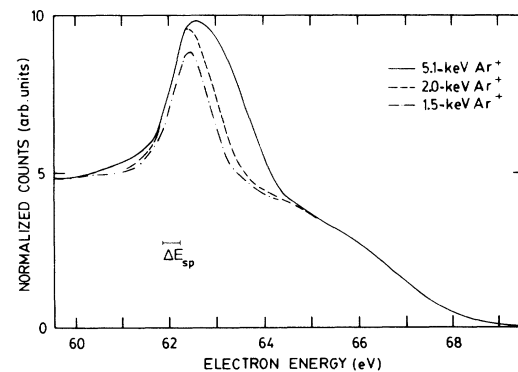


FIG. 4. Auger spectra of Al under bombardment with Ar ions at different energies. The spectra were normalized at an electron energy of 60 eV. Notice that the atomic lines broaden asymmetrically to high electron energies with increasing projectile energy.

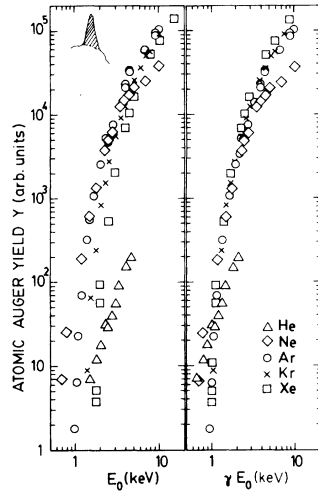


FIG. 5. Yields Y of the main Auger line of Al vs E_0 , the energy of the projectile, and vs γE_0 , the maximum energy transfer in a projectile-Al collision.

III. DISCUSSION

A. The inner-shell excitation collision

One of the questions is whether the inner-shell excitations are produced in collisions involving the projectile and a target atom (PT) or between a fast recoiling target atom and another, most likely stationary, target atom (TT).

If TT collisions dominate, it can be shown²⁵ that the yields Y should follow a universal curve at low energies, when plotted as functions of γE_p . A similar scaling was proposed by Wittmaack²⁶ in which Y/S , where S is the sputtering yield, rather than Y is plotted as a function of γE_p . We feel that this procedure and similar considerations²⁷ are misleading since a typical collision cascade leading

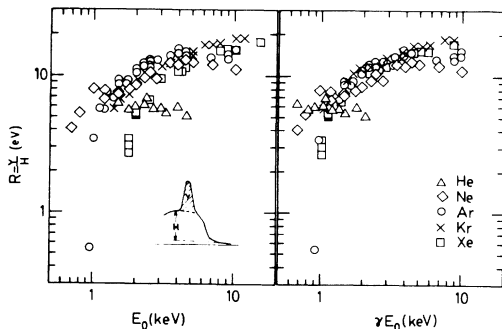


FIG. 6. Ratio R of the yields Y of the main atomic Auger line of Al to H, the bulk line at 60 eV, vs E_0 , the energy of the projectile, and vs γE_0 , the maximum energy transfer in a projectile-Al collision.

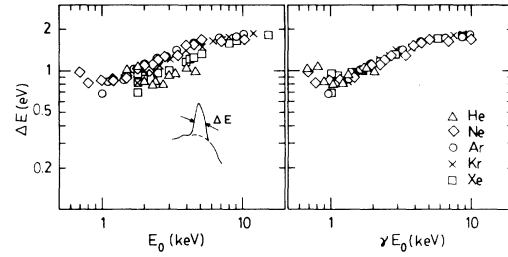


FIG. 7. Full width at half maximum ΔE of the main Auger line of Al vs E_0 , the energy of the projectile, and vs γE_0 , the maximum energy transfer in a projectile-Al collision. The resolution of the analyzer was 0.4 eV FWHM in these measurements.

to sputtering is by no means a typical one leading to violent inner-shell excitation collisions. It can be seen in Figs. 5–7 that the use of the scaled energy γE_p leads to universal curves for Y , R , and ΔE , with good accuracy, except for He^+ and low-energy Ne^+ projectiles. For the other ions, Fig. 8 shows that the low-energy behavior follows a law:

$$Y = Y_0 \left[\frac{\gamma E_p}{E_t} - 1 \right]^p,$$

with $p=2.5$ and $E_t=(0.90\pm 0.02)$ keV. The threshold energy E_t is the minimum energy needed by an Al atom to excite a $2p$ electron in an Al-Al collision. The existence of this threshold is not inconsistent with the idealized electron promotion model of Cacak *et al.*²⁸ In this model, the excitation probability as a function of internuclear distance r is taken as constant below a critical dis-

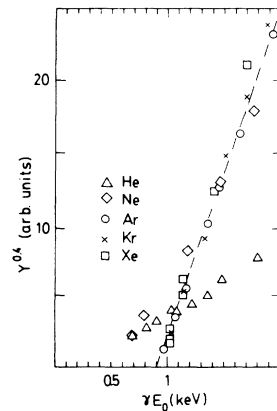


FIG. 8. Near-threshold behavior of the yields Y of the main Auger line of Al vs γE_0 , the maximum energy transfer in a projectile-Al collision. The line represents the fit $Y \propto (\gamma E_0 - 0.9 \text{ keV})^{2.5}$.

tance r_c and zero for $r > r_c$. The critical distance is that at which the promoted electron [in our case in the $4f\sigma$ molecular orbital (MO)] is transferred to an unfilled level.

From the measured value of E_i and calculated²⁹ interatomic potential energy curves for Al₂, we can derive $r_c = 0.53 \text{ \AA}$, in good agreement with theoretical predictions²⁹ for the crossing of the $4f\sigma$ and $3p\pi$ MO's.

For He⁺ and low energy Ne⁺ projectiles, the deviation from the otherwise universal Y vs γE curve indicates that different, projectile-target excitation collisions prevail. These excitations are extremely unlikely, however, in the one-electron transitions of the MO promotion model. Two electron transitions seem possible, perhaps involving molecular states of He⁺Al, He²⁺Al, and He⁺Al⁺($2p^{-1}$) (and the corresponding ones for Ne). We must await detailed calculations of molecular-state curves to draw more conclusions on this mechanism.

B. Identification of the atomic lines

We assign peaks P_1 , P_2 , and P_3 to Auger transitions of sputtered atoms in initial states Al⁰($2p^5 3s^2 3p^2$) and Al⁺($2p^5 3s^2 3p$). These transitions have energies which can be calculated to be close to the ones observed. In particular, the main line is assigned to the transition Al⁰($2p^6 3s^2 3p^2$) → Al⁺($2p^6 3s 3p$). The peak position is 6.29 ± 0.1 eV, after correcting for the difference between the measured work function of the spectrometer and 4.26 eV, the work function of clean polycrystalline Al.³⁰ The calculated Auger energy³¹ is 63.6 eV with an estimated uncertainty of 1 eV, for the most probable (higher multiplicity) $J = \frac{3}{2}$ initial vacancy and ³P final configuration of the outer electrons. Other final Al⁺ states are the $3s3p^1P$, $3p^2$, and $3s^2$ with estimated energies in the regions of the low-energy shoulder of peak P_1 , peak P_2 , and the high-energy edge of the $L_{2,3}VV$ bulk peak, respectively. The intensity of this last transition is expected to be weak.²³

Peaks P_2 and P_3 can be assigned to the initial state Al⁺($2p^5 3s^2 3p$) leading to the final states Al²⁺($2p^6 3s$) and Al²⁺($2p^6 3p$), respectively. The energies estimated by Dahl *et al.*³¹ for these transitions are 57.8 eV and 51.3 eV, respectively, or about 2.5-eV higher than our measured peak energies. Other estimates can be made which yield better agreement with experiment³³ but the uncertainties associated with estimating the energy of the initial level, and the lack of precision electron

excited Auger spectra of free Al atoms, prevents us from drawing more definitive conclusions at present.

We must mention that attempts have been made in the past to assign peaks P_2 and P_3 to discrete energy losses suffered by electrons, originally from peak P_1 , in exciting surface and volume plasmons of Al.³⁴⁻³⁹ A close examination shows, however, that the energy differences are quite removed from the values for those excitations, and that the widths are too small. Vrakking and Kroes⁴⁰ went to the extreme of postulating a decrease in the plasmon frequency of Al by a factor of 2 in the region of the collision cascade in the solid, in order to fit the experiment to the idea of plasmon losses. Still within the model of discrete energy losses is the proposal of Benazeth *et al.*^{41,42} of excitation of $3s$ electrons of the target. These authors had abandoned the idea of plasmon losses after observing that the peak positions did not vary in going from the pure element to alloys. They could not explain, however, the nature of the sharp state to which the $3s$ electron must go; the reason why the $3s$ electron decouples from the band to form a "quasiatomic" level; nor why the energies do not depend on the alloying of the Al samples.

We also disagree with the hypothesis presented by Benazeth *et al.*^{18,42} that the Auger peaks originate from atoms decaying inside the solid, with their valence electrons "decoupled" from the valence band due to the motion of the recoiling nucleus. In fact, even the fastest recoils move with velocities of the order of, or less than, one-tenth the Fermi velocity of Al, and so this motion is nearly adiabatic for the electronic system. A further argument supporting the view that the atomic lines are due to atoms decaying outside the solid will be presented below when discussing the widths of the lines.

C. Line broadening

Different causes of line broadening can be identified, besides normal lifetime broadening, which is negligible for the atomic $L_{23}VV$ lines.³² It is possible that two, or more, different Auger transitions overlap and cause an apparent line broadening. In particular, the 0.4-eV splitting of the $2p_{1/2}$ and $2p_{3/2}$ hole states is unresolved in our experiment. This type of effect, however, is unlikely to have the pronounced dependence on ion energy shown in Fig. 7.

The proximity of the surface of the metal to the decaying atom is another source of broadening. The electronic structure of the atom as it leaves the solid through the surface, evolves from that of the bulk to that of a free atom: the energy levels shift and become narrower as the screening and electronic overlap with other atoms decrease. This source of broadening will be less important as the ion energy increases (in our energy range) since the excited sputtered atoms, carrying increasing mean velocities, decay on the average at larger distances from the surface. This is just opposite the behavior shown by the data (Fig. 7). Thus this effect is not considered to play an important role in our experiments, except, perhaps, at the lowest impact energies. Quantitative conclusions must await knowledge of the energy and angular distribution of the excited sputtered atoms and of their lifetime (which in turn may depend on the distance of the atom to the surface).

The most likely cause of broadening is the distribution in Doppler shifts due to the distribution of velocity components of the decaying atoms in the direction of observation. The Doppler shift is given by

$$\Delta E = 2(E_{\text{eq}}^t E_e)^{1/2} + E_{\text{eq}}^t,$$

with

$$E_{\text{eq}}^t = \frac{m}{M} E \cos^2 \theta,$$

where m is the mass of the electron, M that of the decaying atom, E_e is the electron energy in the frame moving with the atom, E is the kinetic energy of the excited atom at the time of Auger decay, and θ the angle between the directions of motion of the atom and of the electron. For the main atomic line of Al, $\Delta E \simeq 0.07 \text{ eV} \sqrt{E(\text{eV})} \cos \theta$. The Doppler broadening has been proposed before to account for linewidths.^{19,23,33} In past experiments, however, the electron spectrometers collected electrons over a wide range of angles, and it was not possible to draw conclusions regarding the velocity distribution of decaying atoms. In this work, in which the direction of observation is fixed and close to the surface normal, we are able to obtain the distribution of velocities perpendicular⁴³ to the surface of the decaying atoms. The asymmetry of the distributions, and the fact that the low-energy side of the peaks is essentially unaffected by a change in impact energy, suggests that all decaying atoms are moving with velocity components *towards* the analyzer. This provides further support

to our assertion that the atomic peaks originate from sputtered atoms, since one can expect that although atoms decaying in the bulk, near the surface, may have *average* perpendicular velocities towards the surface, they may decay with a sizable probability of moving away from the surface and contribute to an impact energy-dependent broadening of the low-energy side of the peaks.

D. Bulk $L_{2,3}VV$ transitions

After the violent inner-shell excitation collision, the excited Al atom can decay inside the solid, with a lifetime of⁴⁴ $\sim 2 \times 10^{-14}$ sec. This lifetime is much shorter than the value for free atoms³² ($\sim 2 \times 10^{-13}$ sec) due to the increased local electron density in the metal caused by extra-atomic screening. Thus, bulk-Auger transitions occur during the development of the atomic collision cascade in the solid, and therefore, they sample this disordered region. The similarity between ion and electron-excited $L_{2,3}VV$ spectra suggest that this collision cascade is dilute and of small influence to the local density of states in the valence band. The differences can probably be accounted for, at least partially, by Doppler, nonadiabatic,⁴⁵ and collisional broadening.

R , the ratio of atomic to bulk-Auger intensities shown in Fig. 6, is a measure of the chance that a $2p$ -excited Al atom decays outside, rather than inside, the solid. The energy dependence of this ratio can be explained by the fact that, the larger the ion energy, the larger the mean energy of the excited atoms and the larger the chance that they survive as excited during transit to the surface and that they decay outside, rather than inside, the solid.

IV. CONCLUSIONS

Summarizing, our study of Al $2p$ excitation in low-energy ion-surface collisions have led to the following main conclusions:

(1) For heavy-ion impact, single Al $2p$ excitation is produced in a two-step process: a fast recoiling Al atom is produced in a collision between the projectile and a target atom; this recoil then produces the excitation of a $2p$ electron in a violent collision with another Al atom. The excitation occurs by coupling between the $4f\sigma$ and $3p\pi$ orbitals of the Al_2 pseudomolecule formed transiently in the colli-

sion. A threshold center-of-mass energy of 450 eV is required to reach the crossing of the intervening molecular orbitals.

(2) For He^+ and low-energy Ne^+ ions, Al $2p$ excitation occurs in projectile-Al collisions, possibly as a result of two-electron transitions.

(3) The prominent atomic Auger lines originate in sputtered, $2p$ -excited Al atoms and ions. The lines are broadened by the Doppler effect and possibly also by the surface interaction.

Finally, we point out problems which look interesting for future scrutiny: (a) the extraction of information on the valence band, in the region of the collision cascade, from analysis of details of the bulk-Auger transitions; (b) the derivation of the

lifetime of the $2p$ level from the line shapes, and from ratios of atomic to bulk-Auger yields; (c) the relative role of different broadening mechanisms; and (d) the effect of the surface interaction in determining the relative population of the different outer levels of the sputtered, $2p$ -excited, Al particles.

ACKNOWLEDGMENTS

We thank Mario Jakas and Nikolaus Stolterfoht for useful discussions. This work was partially supported by the Secretaría de Estado de Ciencia y Tecnología and by the International Atomic Energy Agency.

*Comisión Nacional de Energía Atómica.

†Comisión Nacional de Energía Atómica and Universidad Nacional de Cuyo.

¹E. S. Parilis and L. Kishinevskii, *Sov. Phys.-Solid State* **3**, 885 (1960).

²R. A. Baragiola, E. V. Alonso, and A. Oliva-Florio, *Phys. Rev. B* **19**, 121 (1979).

³R. A. Baragiola, E. V. Alonso, J. Ferrón, and A. Oliva-Florio, *Surf. Sci.* **90**, 245 (1979).

⁴E. V. Alonso, R. A. Baragiola, J. Ferrón, M. Jakas, and A. Oliva-Florio, *Phys. Rev. B* **22**, 80 (1980).

⁵J. Ferrón, E. V. Alonso, R. A. Baragiola, and A. Oliva-Florio, *J. Phys. D* **14**, 1707 (1981).

⁶C. Snoek, R. Geballe, W. F. van der Weg, P. K. Rol, and D. J. Bierman, *Physica (Utrecht)* **31**, 1553 (1965).

⁷U. Fano and W. Lichten, *Phys. Rev. Lett.* **14**, 627 (1965).

⁸P. Joyes and R. Castaing, *C. R. Acad. Sci.* **263**, 384 (1966).

⁹J.-F. Hennequin, P. Joyes, and R. Castaing, *C. R. Acad. Sci.* **265**, 312 (1967).

¹⁰J.-F. Hennequin, *J. Phys. (Paris)* **29**, 1053 (1968).

¹¹P. Joyes and J.-F. Hennequin, *J. Phys. (Paris)* **29**, 483 (1968).

¹²P. Joyes, *J. Phys. (Paris)* **30**, 243 (1969).

¹³P. Joyes, *J. Phys. (Paris)* **30**, 365 (1969).

¹⁴L. M. Kishinevskii, E. S. Parilis, and V. K. Verleger, *Radiat. Eff.* **29**, 215 (1976).

¹⁵R. A. Baragiola, *Abstracts of the VII International Conference on Atomic Collisions in Solids* (Moscow University, Moscow, 1977), p. 151.

¹⁶R. A. Baragiola, P. Ziem, and N. Stolterfoht, *J. Phys. B* **9**, L447 (1976).

¹⁷J. D. García, R. J. Fortner, H. C. Werner, D. Schneider, N. Stolterfoht, and D. Ridders, *Phys. Rev. A* **22**,

1884 (1980).

¹⁸C. Benazeth, N. Benazeth, and L. Viel, *Surf. Sci.* **65**, 165 (1977).

¹⁹C. Benazeth, N. Benazeth, and L. Viel, *Surf. Sci.* **78**, 625 (1978).

²⁰C. J. Powell, R. J. Stein, P. B. Needham, Jr., and T. J. Driscoll, *Phys. Rev. B* **16**, 1370 (1977).

²¹Equipment made by VG Scientific, England.

²²J. A. Simpson and C. E. Kuyatt, *J. Appl. Phys.* **37**, 3805 (1966).

²³D. E. Ramaker, J. S. Murday, and N. H. Turner, *J. Electron Spectrosc. Relat. Phenom.* **17**, 45 (1979).

²⁴E. N. Sickafus, *Surf. Sci.* **100**, 529 (1980).

²⁵M. M. Jakas and R. A. Baragiola (unpublished).

²⁶K. Wittmaack, *Surf. Sci.* **85**, 69 (1979).

²⁷M. Iwami, S. C. Kim, Y. Kataoka, T. Imura, A. Hiraki, and F. Fujimoto, *Jpn. J. Appl. Phys.* **19**, 1627 (1980).

²⁸R. K. Cacak, Q. C. Kessel, and M. E. Rudd, *Phys. Rev. A* **2**, 1327 (1970).

²⁹N. H. Sabelli, R. Benedek, and T. L. Gilbert, *Phys. Rev. A* **20**, 677 (1979).

³⁰H. B. Michaelson, *J. Appl. Phys.* **48**, 4729 (1977).

³¹P. Dahl, M. Rødbro, G. Hermann, B. Fastrup, and M. E. Rudd, *J. Phys. B* **9**, 1581 (1976).

³²D. L. Walters and C. P. Bhalla, *Phys. Rev. A* **4**, 2164 (1971).

³³W. A. Metz, K. O. Legg, and E. W. Thomas, *J. Appl. Phys.* **51**, 2888 (1980).

³⁴L. Viel, N. Colombie, B. Fagot, and C. Fert, *C. R. Acad. Sci. B* **271**, 239 (1970).

³⁵L. Viel, C. Benazeth, B. Fagot, F. Louchet, and N. Colombie, *C. R. Acad. Sci. B* **273**, 30 (1971).

³⁶C. Benazeth, L. Viel, and N. Colombie, *Surf. Sci.* **32**, 618 (1972).

- ³⁷F. Louchet, L. Viel, C. Benazeth, B. Fagot, and N. Colombie, *Radiat. Eff.* **14**, 123 (1972).
- ³⁸N. Colombie, C. Benazeth, J. Mischler, and L. Viel, *Radiat. Eff.* **18**, 251 (1973).
- ³⁹J. T. Grant, M. P. Hooker, R. W. Springer, and T. W. Haas, *J. Vac. Sci. Technol.* **12**, 481 (1975).
- ⁴⁰J. J. Vrakking and A. Kroes, *Surf. Sci.* **84**, 153 (1979).
- ⁴¹C. Benazeth, L. Viel, and N. Colombie, *C. R. Acad. Sci. B* **276**, 863 (1973).
- ⁴²L. Viel, C. Benazeth, and N. Benazeth, *Surf. Sci.* **54**, 636 (1976).
- ⁴³The small (15°) difference between the direction of observation and the surface normal is unimportant here ($\cos 15^\circ = 0.97$).
- ⁴⁴P. H. Citrin, G. K. Wertheim, and M. Schlüter, *Phys. Rev. B* **20**, 3067 (1979).
- ⁴⁵H. D. Hagstrum, *Phys. Rev.* **139**, A526 (1965). This effect may account for the tail in the high-energy side of the bulk-Auger structure.